JOC The Journal of Organic Chemistry

Article

Cite This: J. Org. Chem. 2019, 84, 2556−2567

pubs.acs.org/joc

Extended Triangulenium Ions: Syntheses and Characterization of Benzo-Bridged Dioxa- and Diazatriangulenium Dyes

Martin Rosenberg,[†] Marco Santella,[†] Sidsel A. Bogh, Alberto Viñas Muñoz, Helene O. B. Andersen, Ole Hammerich, Ilkay Bora, Kasper Lincke, and Bo W. Laursen*

Nano-Science Center and Department of Chemistry, University of Copenhagen, Universitetsparken 5, Copenhagen 2100, Denmark

Supporting Information

ABSTRACT: The very limited class of fluorophores, with a long fluorescence lifetime (>10 ns) and fluorescence beyond 550 nm, has been expanded with two benzo-fused triangulenium derivatives and two cationic [5]-helicene salts. The syntheses of the benzo-bridged dioxa- and diazatriangulenium derivatives (BDOTA$^+$ and BDATA$^+$, respectively) required two different synthetic approaches, which reflect the structural and physiochemical impact on the reactivity of [5]-helicenium precursors. Spectroscopic investigations show that the introduction of the benzo bridge into the triangulenium chromophore significantly redshifts the absorption and emission while maintaining fluorescence lifetimes above 10 ns. The combination of a high quantum yield, long fluorescence lifetime, and emission above 600 nm is possible only if the structural aspects of the triangulenium framework are perfectly harmonized to secure a low rate of nonradiative deactivation. The new benzo bridge may be a general motif to obtain red-shifted derivatives of other dye classes.

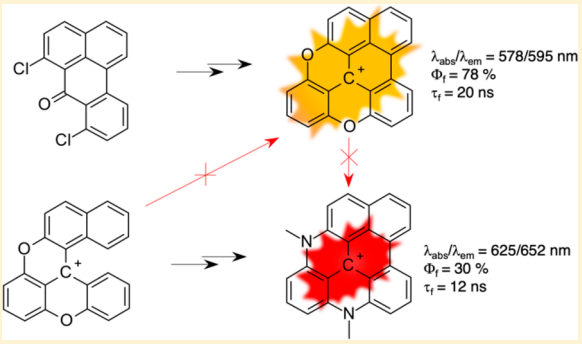

INTRODUCTION

Organic fluorophores are essential tools in life science, and many of the commercially available fluorophores are based on the fluorescein and rhodamine motifs.[1] In the past decade, considerable interest has been targeted at exploring how structural modulations in these classical fluorophores affect the optical properties. Special attention has been devoted to structural designs where the xanthene oxygen bridge in the rhodamine, fluorescein, and rhodol scaffolds has been exchanged with silicon,[2−16] phosphor,[17−20] sulfur,[21] and carbon[15,17,22−26] bridges. These structural modifications shift the absorption and fluorescence of these bright fluorophores to the red and near-infrared parts of the spectrum. This makes them especially attractive as probes and labels for fluorescence microscopy investigations of biological systems, as the fluorescence signal in this spectral region can be detected with a reduced autofluorescence background. Additionally, the red and near-infrared lights have deep penetration in tissue, making these probes applicable for in vivo imaging. The growing interest, in the applications of especially the Si-bridged rhodamine fluorophores, has led to extensive investigations of various synthetic strategies to introduce such structural modifications.[10,12,13,27,28] The unprecedented brightness of the rhodamine- and fluorescein-type dyes makes them obvious choices as probes and labels for fluorescence microscopy applications. However, their fluorescence lifetimes are typical in the 1−5 ns range, limiting their use for applications such as fluorescence lifetime bioassays and imaging (FLIM),[29,30] time-gated detection,[31] and polarization assays.[32] Only a limited number of organic fluorophores with emission in the visible range and fluorescence lifetimes above 5 ns have been reported.[29,32,33] The triangulenium salts are a class of compounds, which among others, include the chemically stable azadioxatriangulenium and diazaoxatriangulenium derivatives, ADOTA$^+$ and DAOTA$^+$ (Figure 1).[34,35]

These two derivatives fluoresce in the 550−600 nm range with high fluorescence quantum yields ($\Phi_f \approx 0.7-0.8$) and

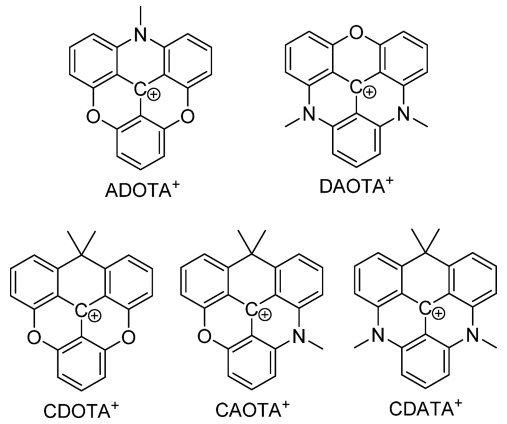

Figure 1. Structures of key aza/oxa triangulenium compounds. Anions are omitted for clarity.

Received: November 22, 2018
Published: January 29, 2019

DOI: 10.1021/acs.joc.8b02978
J. Org. Chem. 2019, 84, 2556−2567

long fluorescence lifetimes (close to 20 ns).[36] The combination of long fluorescence lifetimes and high quantum yields has proven them to be particularly good fluorescent probes in FLIM and time-gated fluorescence imaging,[30,31,37,38] and for fluorescence lifetime and polarization assays.[37,39−42] Recently, we reported triangulenium dyes where one aza/oxa bridge is exchanged with a saturated isopropyl bridge, as in CDOTA$^+$, CAOTA$^+$ and CDATA$^+$ (Figure 1).[43] In similarity to the rhodamine fluorophores, the introduction of the carbon bridge in the triangulenium chromophore resulted in a significant redshift of the absorption (λ_{abs}) and fluorescence (λ_{em}) intensities, when comparing the carbon-bridged CDATA$^+$ ($\lambda_{abs}/\lambda_{em}$= 603/624 nm) with the oxygen-bridged DAOTA$^+$ ($\lambda_{abs}/\lambda_{em}$= 555/575 nm).[36,43] CDATA$^+$ preserves a good quantum yield (61%), a long fluorescence lifetime (∼16 ns), and a high photostability, and it showed a promising performance as a fluorescent dye in time-gated fluorescence detection.[43] In the pursue of further redshifting the absorption and emission properties of triangulenium fluorophores, the introduction of bridges similar to those described for the rhodamine analogous would seem to be the obvious next targets. However, the results of the structural and spectroscopic analyses of CDATA$^+$ vs DAOTA$^+$ indicated that the introduction of the carbon bridge enhanced the nonradiative deactivation of the fluorophore, when compared to DAOTA$^+$. The enhanced nonradiative deactivation was assigned to the sp^3-hybridized carbon bridge, which can provoke nonplanar configurations to release the ring tension induced by the longer CC bond lengths. Thus, it is suspected that an introduction of groups with even longer bond lengths in the bridge such as C−Si, C−P, and C−S bonds may lead to an undesired enhanced nonradiative deactivation of the triangulenium fluorophore. Instead, we consider a triangulenium design involving a more rigid carbon bridge and shorter CC bonds, when compared to the sp^3-hybridized carbon bridge. A conjugated bridge fulfills these criteria and can be introduced via fusion of a benzene ring in the triangulenium skeleton as shown in Figure 2. This

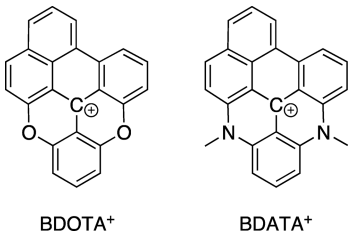

Figure 2. Benzo-bridged dioxa- and diazatriangulenium derivatives, BDOTA$^+$ and BDATA$^+$, respectively. The anions are omitted for clarity.

bridge motif has to our knowledge not previously been explored in xanthenium-like fluorophores and could be a general motif for extension and modification of, e.g., fluorescein and rhodamine-like dye-systems. In this work, different synthetic strategies for introducing this benzo-fused bridging motif in the triangulenium system are explored. The benzo-bridged dioxa- and diazatriangulenium derivatives BDOTA$^+$ and BDATA$^+$ are investigated by optical spectroscopy, electrochemistry, and computations to elucidate how this bridging motif impacts the properties of the triangulenium system.

RESULTS AND DISCUSSION

Synthesis. The introduction of the benzo-fused bridge in the triangulenium structure was explored by two different synthetic strategies as depicted in Scheme 1 and Scheme 2.

Scheme 1. Synthetic Route to the Benzodioxatriangulenium Derivative 4[a]

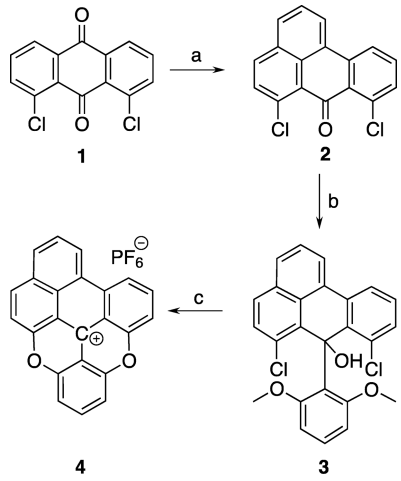

[a]Reaction conditions: (a) (1) Al, H_2SO_4, 25 °C, 18 h, (2) glycerol, H_2SO_4, 125 °C, 3.5 h, 44%; (b) benzene, diethyl ether, *n*-BuLi, 1,3-dimethoxybenzene, 20 °C, 1 h, 27%; (c) (1) 48% $HBr_{(aq)}$, AcOH, reflux, 48 h, (2) 0.2 M $KPF_{6(aq)}$, 42%.

The route via the benzanthrone derivative (**2**) was inspired by the previously reported strategies for preparations of sulfur- and carbon-bridged triangulenium salts,[43,44] where the alternative bridge is introduced prior to the formation of the triangulenium scaffold containing oxygen/nitrogen bridges.

Compound **2** was prepared from 1,8-dichloroanthraquinone (**1**) using the analogous two-step/one-pot procedure for preparation of benzanthrone, involving a reduction with metallic copper in H_2SO_4 followed by a Skraup-type condensation with glycerol.[45,46] Following this method, **2** was isolated in a maximum 20% yield, and only poor conversion of the starting material was achieved, even when freshly activated copper metal was used. Thus, instead the reduction of **1** was performed with aluminium metal according to the procedure described by House et al.[47] Following this procedure, complete conversion of **1** was obtained, giving a crude mixture of the 7,11-dichloroanthrone and 4,5-dichloroantrone isomers as the dominant products in 75:25 internal ratio, as determined by the results of ^{1}H NMR analysis. The mixture of the two isomers was reacted with glycerol in H_2SO_4 to yield **2** in 44% yield, after purification via column chromatography. Compound **2** was converted into the carbinol **3** in 27% yield, by reaction with *ortho*-lithiated 1,3-dimethoxybenzene in benzene/ether[48] at ambient temperature. The corresponding carbenium ion of **3** was prepared by dehydration of **3** with aqueous HBF_4, and was isolated in 92% yield by precipitation as the tetrafluoroborate salt (**3a**, Supporting Information). However, this compound proved to degrade after a short time of storage, and attempts to introduce nitrogen bridges at this stage by reaction of **3a** with primary amines as common to triangulenium synthesis[34] led to immediate decolorization of the reaction mixture. The results of MALDI-TOF analysis showed no signs of substitutions of

DOI: 10.1021/acs.joc.8b02978
J. Org. Chem. 2019, 84, 2556−2567

Scheme 2. Synthetic Routes to the Benzodiazatriangulenium Derivative 14[a]

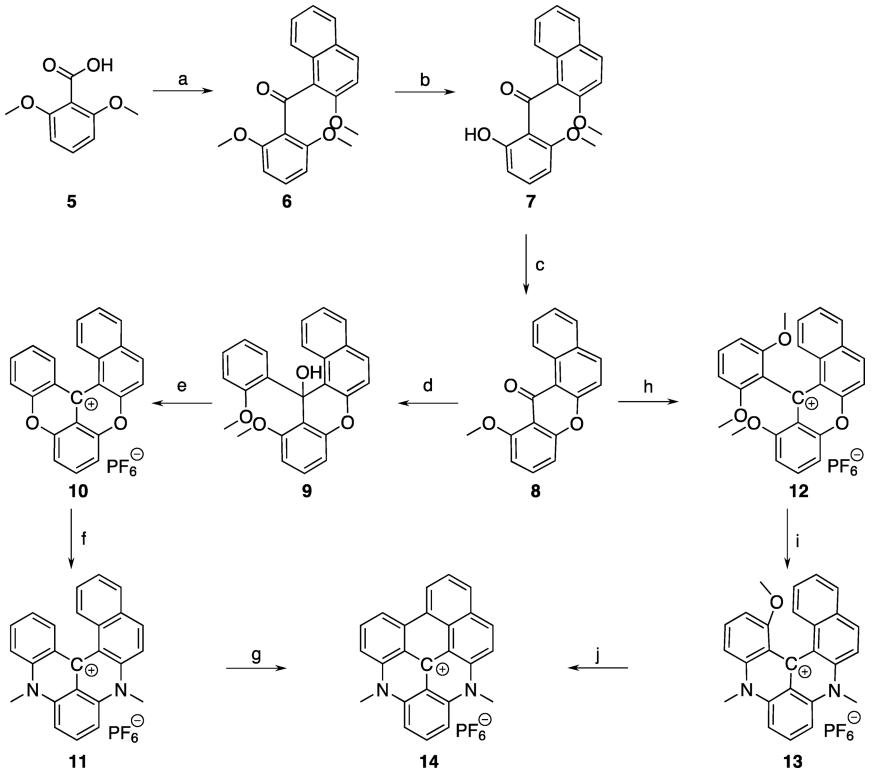

[a]Reaction conditions: (a) (1) $SOCl_2$, $PhCH_3$, 3 h, 65 °C; (2) 2-methoxynaphtalene, $AlCl_3$, CH_2Cl_2, 0 °C, 2 h 63%; (b) BBr_3, −78 → 25 °C, CH_2Cl_2, 3 h, 82%; (c) neat, 225 °C, 5 h, 64%; (d) benzene, Et_2O, 2-bromoanisole, Li, reflux, 30 min, 88%; (e) pyridine HCl, 190 °C, 5 min, 44%; (f) $PhCO_2H$, 33% NH_2CH_3 in absolute EtOH, NMP, 90−95 °C, 12%; (g) PPA, 110 °C, 30 h, 33%; (h) (1) benzene, Et_2O, TMEDA, 1,3-dimethoxybenzene, *n*-BuLi, reflux, 48 h; (2) 6 M $HCl_{(aq)}$, 0.2 M $KPF_{6(aq)}$, 47%; (i) $PhCO_2H$, 33% NH_2CH_3 in absolute EtOH, NMP, 90−95 °C, 12%; (j) PPA, 110 °C, 1 h, 36%.

either the chlorine atoms of methoxy groups even upon addition of excess quantities of an amine, elevated reaction temperatures, or extended reactions times. This is most likely due to irreversible formation of the leuco adduct as it has been observed by Lacour and co-workers for sulfur-bridged cations.[44] Thus, the alternative strategy where the amine bridges are introduced via the more chemically stable ring-closed dioxatriangulenium derivative was explored.[34,43,49] Compound **4** was prepared from **3** by in situ dehydration followed by cleavage of the methoxy groups and intramolecular aromatic substitution in a refluxing mixture of 48% aqueous HBr and acetic acid. After ion exchange, the benzodioxatriangulenium derivative **4** was isolated as the hexafluorophosphate salt in 42% yield. In contrast to the preparation of other triangulenium derivatives,[34,44,50] attempts to obtain **4** via reaction in melted pyridine hydrochloride was ineffective in comparison to the latter conditions. In an attempt to substitute the oxygens with nitrogen bridges, compound **4** was reacted with methylamine, *n*-propylamine, or *n*-octylamine using previously described reaction conditions.[34] However, oxygen substitutions were not observed. Instead, according to the results of MALDI-TOF analysis of the reaction mixture, the reaction of **4** and the various primary amines exclusively led to reaction products arising from substitution in the CH aromatic positions within short reaction times. Such substitutions employing aliphatic amines have also been reported for [6]-diazahelicenium ions.[51,52] In the pursuit to synthesize the benzodiazatriangulenium ($BDATA^+$) derivative, we explored two other routes (Scheme 2), which were inspired by the synthetic route toward [6]-helicenium ions, with the part toward compound **8** being similar to that reported by Lacour and co-workers.[51,52]

Instead of the reported two-step procedure,[51,52] compound **6** was prepared by a one-pot Friedel−Crafts acylation of 2-methoxynaphtalene with 2,6-dimethoxybenzoyl chloride. Compound **6** was subsequently converted into the xanthone derivative **8** as previously described.[52] From this compound, two routes via the [5]-helicenium ions **10**, **11**, and **13** were examined. The carbinol **9** was obtained in 88% yield, via nucleophilic addition of lithiated 2-bromo-anisole to **8**. Dehydration of carbinol **9** through reaction with aqueous HBF_4 lead to an unstable carbenium ion, as described for **3**, from which we were unable to obtain useful products by reaction with primary alkyl amines. The reaction of **8** with *ortho*-lithiated 1,3-dimethoxybenzene was performed under similar conditions as described to give **9**. However, this addition reaction required longer reaction times and elevated temperatures to progress to completion, and the carbinol product was difficult to isolate. In contrast to **9**, in situ dehydration of the carbinol with aqueous HCl, followed by ion exchange, easily gave the carbenium ion **12.** This carbenium ion is a stable compound, which can be stored without special precautions. In fact, it was possible to introduce two nitrogen bridges by nucleophilic aromatic substitution of **12** with excess methylamine in 18 h reaction time under buffered conditions, giving the methoxy substituted diaza[5]-helicenium derivative **13** in 12% yield. To investigate whether oxygen ring closure of **9** would allow for a more effective introduction of amine

DOI: 10.1021/acs.joc.8b02978
J. Org. Chem. 2019, 84, 2556−2567

bridges, the dioxa[5]-helicenium **10** was prepared. Compound **10** was easily isolated in 44% yield after 5 min of reaction of **9** in melted pyridine hydrochloride at 190 °C. This cationic dioxa[5]-helicene was stable upon extended storage, and it was possible to obtain the diaza[5]-helicenium compound **11**, by reaction with methylamine under buffered conditions. However, as for the reaction of **12** to **13**, only a poor reaction yield of 12% was achieved. We have not yet been able to identify the excessive amounts of byproducts formed by competitive or degradation reactions. However, the results of MALDI-TOF analysis during the reaction of **10** to **11** did not show signs of substitution in the aromatic positions as described for the BDOTA$^+$ derivative **4**. Thus, the twisted geometry of **10** tends to alter the regioselectivity of the amine substitution, in comparison to the selectivity observed for the planar BDOTA$^+$ derivative **4**. With compound **11** in hand, different conditions were screened for fusing the ring system of **11** via an intramolecular oxidative aromatic coupling[53] to yield the BDATA$^+$ derivative **14**. Reactions with $FeCl_3$ and $AlCl_3$ neat or in solutions were unsuccessful. However, inspired by the conditions reported by Pieters et al.,[54] compound **14** was obtained from **11** in polyphosphoric acid (PPA) at 110 °C in 30 h. This approach yielded **14** in 33% yield with simple purification. When **13** was exposed to PPA at 110 °C, the reaction time was significantly reduced, with **13** being converted into **14** in 1 h in a comparable yield of 36%. Acidic conditions have also been used in the preparation of a similar compound described by Suenaga et al.,[55] in which the methoxy group had been introduced to achieve an efficient coupling of two aromatic moieties. The experimental results inspired us to investigate whether the BDOTA$^+$ derivative, **4**, could also be prepared directly from **12** under acidic ether cleaving reaction conditions. Cleavage of all three methoxy groups was surprisingly challenging, and the exposure of **12** to melted pyridine hydrochloride led to extensive degradation and only partial ring-closed and ether-cleaved reaction products. By reaction of **12** with excess quantities of aqueous HBr in refluxing acetic acid, it was possible to achieve complete ether cleavage and oxygen ring closure in 36 h to obtain compound **15** (Scheme 3), although in a very low yield (7%). No trace of

Scheme 3. Attempted Preparation of 4 from 12[a]

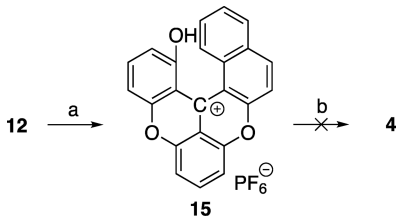

[a]Reaction conditions: (a) 48% $HBr_{(aq)}$, AcOH, reflux, 36 h, 7%; (b) PPA, 110 °C.

4 was observed after exposing **15** to PPA under the conditions that successfully converted **13** into **14**, even for an elongated reaction time. This result is explained by considering the energy required to generate the double cationic Wheland intermediate (σ-complex)[53] in the ring closure of **15**, **11**, and **13**. The oxidation potentials of **11**, **13**, and **10** were measured by differential pulse voltammetry (DPV). The oxidation potential of **10** was measured to be 2.190 V, while for **11** and **13** the oxidation potentials are 1.287 and 1.265 V (see Table 1). The oxidation potential of **15** was not measured due to the very poor solubility of the compound in various

Table 1. Reduction and Oxidation Potentials for Triangulenium Derivatives (4, 14, ADOTA$^+$, DAOTA$^+$, CDOTA$^+$, CAOTA$^+$, and CDATA$^+$) and the Helicenium Derivatives (10, 11, and 13)[a]

compound	E^{ox} (1) [V]	E^{ox} (2) [V]	E^{red} (1) [V]	E^{red} (2) [V]
4 (BDOTA$^+$)	2.060		−0.226	−1.233
10	2.190		−0.121	
CDOTA$^+$			−0.299	
ADOTA$^+$[b]	1.814		−0.559	
CAOTA$^+$	1.723		−0.652	
11	1.287		−0.782	
13	1.265	1.941	−0.799	−1.544
14 (BDATA$^+$)	1.215		−0.874	−1.594
CDATA$^+$	1.290		−0.871	−1.615
DAOTA$^+$[b]	1.108	1.443	−0.958	

[a]Potentials in V vs SCE. [b]Comparable potentials were reported by Dileesh and Gopidas.[57] The formal potentials reported by Adam et al. are however approximately 600 mV higher than ours and appear to be in error.[61]

organic solvents. However, based on the similarity of the oxidations potentials of **11** and **13**, we expect a similar difference between the potentials for **10** and **15**. From the measured potentials, it is clear that the formation of the double cationic intermediate requires significantly more energy in a dioxa[5]-helicenium derivative when compared to the diaza-derivatives. This difference reflects the weaker π-electron-donating properties of the oxygen atoms compared to nitrogen atoms and could explain the failure to ring close **15**.

Electrochemistry. The reduction and oxidation potentials are key parameters to understand the electronic effects of modifying dye systems. Both the ground state stability of the cations and their susceptibility to excited state quenching by photoinduced electron transfer (PET) are intimately linked to the redox potentials.[49,56,57] To elucidate the effects of the conjugated benzo bridge compared to a saturated carbon bridge and aza/oxa bridges, we measured the redox properties of the new benzo-triangulenium ions and their [5]-helicenium precursors. For comparison, we also measured the family of triangulenium ions with saturated bridges (CDOTA$^+$, CAOTA$^+$, CDATA$^+$) not previously reported and ADOTA$^+$ and DAOTA$^+$ (structures are shown in Figure 1).

The redox properties of all of the cationic dyes were studied by cyclic voltammetry and DPV in CH_3CN, containing Bu_4NPF_6 (0.1 M) as the supporting electrolyte. The cyclic voltammograms obtained at a voltage scan rate of 0.1 V s^{-1} are reproduced in the Supporting Information. It is observed that except for the *N*,*N*-dipropyldiazaoxatriangulenium ion (DAOTA$^+$), one-electron oxidation to the radical dications proceeds reversibly for the compounds containing two nitrogen atoms; in all other cases, the radical dications undergo follow-up reactions to products that are further oxidized. One-electron reduction to the neutral radicals was observed to be reversible in all cases except for **4** and **14**, for which one-electron reduction results in two overlapping waves. Similar overlapping waves have been reported for the one-electron oxidation of a number of planar tetrathiafulvalene (TTF) derivatives and were shown to reflect the formation of π-dimers between neutral TTF and its radical cation and/

DOI: 10.1021/acs.joc.8b02978
J. Org. Chem. 2019, 84, 2556−2567

or between two radical cations.[58−60] In analogy, we suggest that the broad waves observed for one-electron reduction of the planar **4** and **14** are caused by the formation of cation−radical and radical−radical π-dimers. Further reduction leads to the formation of the corresponding anions that, only in one case, **4** proceeds as a reversible process, the general trend being the observation of distorted waves that most likely are caused by deposition of insoluble material on the electrode surface. The potentials for oxidation and reduction of **4**, **10**, **11**, **13**, and **14** determined by DPV are summarized in Table 1 together with potentials for the carbon-bridged dioxa-, azaoxa-, and diazatriangulenium derivatives (CDOTA$^+$, CAOTA$^+$, and CDATA$^+$, respectively), and ADOTA$^+$ and DAOTA$^+$. In general, the results show that the compounds with planar configurations have reduced first reduction potentials, when compared to their distorted helicenium equivalents (**4** vs **10** and **14** vs **11** and **13**). This is explained by better delocalization of the π-electrons in the planar configurations. Looking at the diaza cations, it is clear that exchanging the nonaza bridge from oxygen (DAOTA$^+$) to carbon lowers the reduction potential approximately 90 mV, but there is no difference between the saturated (CDATA$^+$) and conjugated benzo (BDATA$^+$) bridge in this regard.

Spectroscopy and Structural Analyses. The optical properties of the BDOTA$^+$ and BDATA$^+$ derivatives **4** and **14**, respectively, and their [5]-helicenium precursors **10**, **11**, and **13** were measured in CH_2Cl_2 solutions. Absorption and emission spectra of BDOTA$^+$ (**4**) and BDATA$^+$ (**14**) are shown in Figure 3. The absorption, emission, and excitation

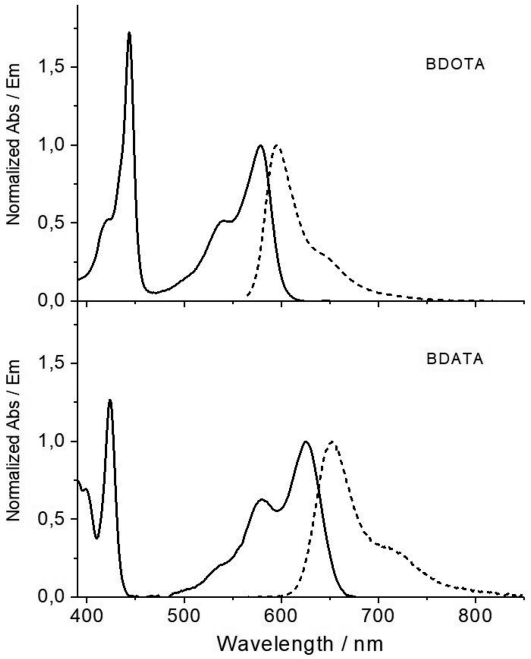

Figure 3. Normalized absorption and emission spectra of BDOTA$^+$ (**4**) and BDATA$^+$ (**14**) in CH_2Cl_2 solution.

spectra of all of the dye compounds can be found in the Supporting Information. The spectroscopic data are listed in Table 2. A first observation in the absorption and emission spectra of the planar benzo-bridged dyes BDOTA$^+$ and BDATA$^+$ is a redshift relative of 40 and 25 nm, respectively, relative to the isopropyl-bridged analogues, CDOTA$^+$ and CDATA$^+$ (Table 2). Furthermore, the characteristic intense and narrow absorption bands at 443 nm (BDOTA$^+$) and at 423 nm (BDATA$^+$) are not seen in the isopropyl-bridged analogues,[43] nor in the [5]helicenium precursors **10**, **11**, and **13** and are assigned to the benzo-bridged motif (see Supporting Information).

Table 2. Photophysical Properties of 4, 10, 11, 13, and 14 Measured in CH_2Cl_2 Solution[a]

compound	λ_{abs} [nm]	λ_{em} [nm]	Φ_f	τ_f [ns]	k_{rad} 10^6 s^{-1}	k_{nr} 10^6 s^{-1}
4 (BDOTA$^+$)	578	595	0.78	20.2	38	11
10	564	600	0.18	6.6	27	125
CDOTA$^+$[b]	535	554	0.54	23.1	23	20
11	614	654	0.31	10.2	30	68
13	613	654	0.35	12.7	28	51
14 (BDATA$^+$)	625	652	0.30	12.2	25	57
CDATA$^+$[b]	603	624	0.61	15.8	39	25

[a]Column list: λ_{abs}, wavelength at the maximum intensity of the $S_0 \rightarrow S_1$ transition; λ_{em}, wavelength at the maximum fluorescence intensity; Φ_f, fluorescence quantum yield; τ_f, fluorescence lifetime; $k_{rad} = \Phi_f/\tau_f$, $k_{nr} = (1/\tau_f) - k_{rad}$. [b]Data taken from ref 43.

When comparing the carbon-bridged dioxatriangulenium derivatives CDOTA$^+$ with BDOTA$^+$ (**4**), it is observed that the quantum yield (Φ_f) for **4** is higher, and its nonradiative rate constant (k_{nr}) is reduced by 40%. These results indicate that the benzo-fused bridge does introduce the desired rigidity in the triangulenium framework. However, for BDATA$^+$ (**14**), an opposite trend is observed; i.e., Φ_f is lower, and k_{nr} is enhanced when compared to CDATA$^+$. The significant nonradiative deactivation of the excited state of **14** emphasizes that the more important structural deformations for this deactivation are associated with the geometry around the nitrogen atoms, in similarity to the DAOTA$^+$ chromophore.[36] This interpretation is supported by inspection of the calculated structures of BDATA$^+$ (**14**) and DAOTA$^+$.[43] The calculated CC bond lengths in the bridge of BDATA$^+$ are 1.43 and 1.47 Å (Supporting Information), which are significantly longer than the CO bond lengths of DAOTA$^+$ (1.37 Å). Despite these differences, comparable deviations from planarity are found, when comparing the calculated structures of BDATA$^+$ and DAOTA$^+$ derivatives (Supporting Information). However, the longer bond lengths in combination with the rigidity of the bridge in BDATA$^+$ presumably makes BDATA$^+$ more prone to the deactivating structural distortions in the excited state around the nitrogen atoms in comparison to DAOTA$^+$. When comparing BDATA$^+$, CDATA$^+$, and DAOTA$^+$, it seems that the optimal relation between structure and optical properties in the diazatriangulenium chromophore rely on a delicate balance between bond lengths and rigidity of the bridging group. The lowest energy absorption bands of the [5]-helicenium derivatives **10** and **11** are similar to those of the corresponding [6]-helicenium derivatives (λ_{abs} = 574 and 619 nm, respectively).[52] Comparison of the results of **11** and **13** reveals that presence of the methoxy group has no significant effect on the positions of λ_{abs} and λ_{em}. However, the difference in nonradiative rate constant reflects the more constrained geometry of **13**, associated with the presence of the methoxy group. Interestingly, the planarization and fusion of the ring system result in a redshift of λ_{abs} (comparing **4** vs **10**, and **11** vs **14**, respectively). This stands in contrast to the general trend for similar dyes systems, where structural deformations from

DOI: 10.1021/acs.joc.8b02978
J. Org. Chem. 2019, 84, 2556−2567

planarity result in a redshift of λ_{abs}.[62] This opposite trend can be explained by Dewar's rules,[62−65] by considering the benzo extension as a butadiene perturbation to the [4]-helicenium derivative **16** (Figure 4). This analysis is applicable, as

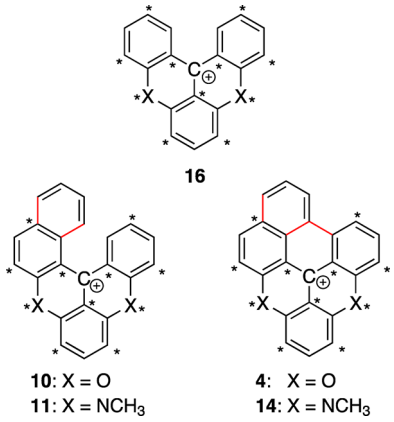

Figure 4. Starring of the [4]helicenium ion **16**. The unions of butadiene to yield the cations of **10**, **11**, **4**, and **14** are marked in red.

inspections of the calculated HOMO and LUMO orbitals and the direction of the transition dipole moments of the $S_0 \rightarrow S_1$ transitions in **4**, **10**, **11**, and **14** (Supporting Information) suggest a similar character of these transitions in the latter compounds.

In this picture, the extension of the conjugated system by four π-electrons will result in equal redshift of $S_0 \rightarrow S_1$ transitions of **4**, **10**, **11**, and **14**, if compared to **16**. Additionally, the butadiene moiety acts as a carbon substituent, which will add a further redshift of the $S_0 \rightarrow S_1$ transition when substituted at nonstarred positions and an opposing blueshift upon substitution at a starred position (see Figure 4).[62−65] For **10** and **11**, the net effect of the carbon substitutions will be zero; while for **4** and **14**, the net result will be an additional redshift due to the extra substitution at a nonstarred position when the benzo bridge is formed. Thus, we propose that the latter introduces a larger redshift on λ_{abs} for **4** and **14**, than the influence of structural deformation on λ_{abs} for **10** and **11**. Beside this moderate redshift upon formation of the benzo bridge when going from [5]-henicenium **10** or **11** to BDATA$^+$ **14**, the effects on quantum yield and fluorescence lifetime are surprisingly small.

The reported derivatives of benzo-bridged triangulenium dyes, BDOTA$^+$ (**4**) and BDATA$^+$ (**14**), are only soluble in organic solvents, due to their planar structure, lack of polar groups, and accompanying the lipophilic PF_6^- counterion. For application of these new redshifted long fluorescence lifetime chromophores in bioassays and bioimaging increased water solubility and reactive groups, for bioconjugation, will have to be built into the structures.

CONCLUSIONS

The classes of triangulenium and helicenium compounds have been expanded with the benzo-bridged dioxa- and diaza-triangulenium derivatives **4** and **14** and the dioxa- and diaza[5]-helicenium derivatives **10**, **11**, and **13**. The synthetic results show that the introduction of the benzo-fused ring hampers the introduction of primary amines through nucleophilic aromatic substitution by opening up routes toward other reaction products. The results of the spectroscopic investigations of **4** and **10** revealed that the rigid bridges are indeed important to achieve a high quantum yield and a long fluorescence lifetime. Despite an undesired decrease of the fluorescence quantum yield and lifetime for the diaza derivative (**14**, BDATA$^+$), the benzo bridge does provide a much desired redshift while retaining a long fluorescence lifetime (τ_f > 10 ns). The benzo bridge may also provide interesting possibilities for redshifting other groups of dyes.

EXPERIMENTAL SECTION

Synthetic Methods and Materials. All chemicals and solvents were purchased from commercial suppliers and used as received. Benzene was dried over metallic sodium for at least 24 h before use. Thin-layer chromatography (TLC) was carried out on commercially available precoated plates (silica 60) with a fluorescence indicator. Chromatographic purifications were performed on silica gel (SiO_2) with a pore size of 60 Å and a particle size of 40−63 μm. Mass spectra were recorded on an ESP-MALDI-FT-ICR instrument equipped with a 7 T magnet (the instrument was calibrated using sodium trifluoroacetate cluster ions prior to acquiring the spectra) or a MicrOTOF-QII-system using ESP (calibrated using formic acid). The spectra were recorded using dithranol as a matrix. All melting points are uncorrected. ^{1}H and ^{13}C NMR spectra were acquired on a Bruker 500 MHz instrument equipped with a (noninverse) cryoprobe. All chemical shift values in ^{1}H and ^{13}C NMR spectra are referenced to the residual solvent peak ($CDCl_3$ δ H = 7.26 ppm, δ C = 77.16 ppm; DMSO-d_6 δ H = 2.50 ppm, δ C = 39.52 ppm; CD_2Cl_2 δ H = 5.32, δ C = 53.84 ppm; CD_3CN δ H = 1.94 ppm, δ C = 1.32 ppm).[66] Elemental analysis was done at the University of Copenhagen, Department of Chemistry, Elemental Analysis Laboratory, Universitetsparken 5, Copenhagen DK-2100, Denmark.

Electrochemistry. Cyclic voltammetry (CV) and differential pulse voltammetry (DPV) were carried out at room temperature in CH_3CN containing Bu_4NPF_6 (0.1 M) as the supporting electrolyte using an Autolab PGSTAT12 instrument driven by the Nova 1.11 software. The working electrode was a circular glassy carbon disk (d = 3 mm), the counter electrode was a platinum wire, and the reference electrode was a silver wire immersed in the solvent-supporting electrolyte mixture and was physically separated from the solution containing the substrate by a ceramic frit. The potential of the reference electrode was determined vs the ferrocene/ferrocenium (Fc/Fc^+) redox couple in separate experiments, and the potentials were subsequently converted to V vs SCE by addition of 0.382 V.[67] The CV voltage scan rate was 0.1 V s^{-1}. The DPV parameters were as follows: scan rate 0.01 V s^{-1}, step potential 0.005 V, modulation amplitude 0.025 V, modulation time 0.05 s, and interval time 0.5 s. *iR*-Compensation was used in all experiments. Solutions were purged with argon saturated with CH_3CN for at least 10 min before the measurements were made, after which a stream of argon was maintained over the solutions. Potentials were determined by DPV. Synthesis and characterization of the used reference compounds can be found elsewhere: propyl derivatives ADOTA$^+$ and DAOTA$^+$ BF_4^- salts[34] and methyl derivatives of CDOTA$^+$, CAOTA$^+$, and CDATA$^+$ PF_6^- salts.[43]

Spectroscopic Methods. Solvents used for spectroscopic measurements were of highest purity grade and used as received. The UV−vis absorption spectra were recorded on a PerkinElmer Lambda 1050 UV/vis/NIR double beam spectrometer using the pure solvent as a baseline. The spectra were recorded in 1 cm path length cuvettes and 1 nm steps. Fluorescence spectra and lifetimes were measured using a FluoTime 300 (PicoQuant, Berlin, Germany) system. The fluorescence decays were analyzed using the FluoFit software package. The decay data ($I_f(t)$) were fitted by iterative reconvolution with a sum of exponentials:

$$I_f(t) = \sum_i \alpha_i \exp(-t/\tau_i) \quad (1)$$

In eq 1, α_i is the amplitude and τ_i is the fluorescence lifetime of the i^{th} component, respectively. The samples were excited using a pulsed

DOI: 10.1021/acs.joc.8b02978
J. Org. Chem. 2019, 84, 2556−2567

solid-state laser with 560 nm excitation. The photons were counted at the maximum emission intensity wavelengths of the samples. The instruments response function (IRF) was measured at the excitation wavelength using a dilute scattering suspension of Ludox. For all fluorescence measurements, the angle between the excitation and emission polarizers was set to 54.7° (magic angle). All fluorescence quantum yields were determined by the relative method.[68] The samples were excited by a pulsed solid-state laser at 560 nm, and the quantum yields were determined with respect to cresyl violet in absolute ethanol (Φ = 0.58).[69] The fluorescence measurements were performed in a 1 cm path length cuvette at a 90° angle with respect to the excitation light. For all quantum yield measurements, the absorbance was below 0.12 at the maximum of the lowest energy absorption band. After each fluorescence measurement, an absorption spectrum was recorded in order to verify that no photobleaching of the sample had occurred during the fluorescence measurement. All fluorescence spectra were corrected for the wavelength-dependent sensitivity of the detection system from 500 to 900 nm.

Computational Methods. All calculations were performed with the Gaussian 09 suite of programs.[70] All computations were performed using the same methods, as described in our previous work, and further details can be found in ref 43.

*Synthesis. 6,8-Dichloro-7H-benzo[de]anthracen-7-one (**2**).* Aluminum metal (1.51 g, 55.9 mmol) and 1,8-dichloroanthraquinone (5.0 g, 18 mmol) were suspended in concentrated H_2SO_4 (150 mL) in a three-necked flask equipped with a mechanical stirrer, a thermometer, and a condenser. The yellow mixture was stirred overnight without applying heat. The mixture was then heated to 85 °C, and a mixture of glycerol (5.2 g, 56 mmol) in water (5 mL) was added dropwise. Upon completion of the addition, the resulting dark red solution was heated to 125 °C with a ramp of 5 °C for every 10 min. When 125 °C was reached, the mixture was stirred for an additional 2 h. Afterward, the red mixture was allowed to reach ambient temperature and then poured onto an ice/water mixture. The fine black precipitate was filtered on a Büchner funnel. The solid was then dissolved in CH_2Cl_2 and adsorbed on Celite by evaporation in vacuo. The material was purified by dry column chromatography (dry load on Celite, heptane/toluene 5% gradient, then toluene/CH_2Cl_2, 2% gradient) followed by recrystallization from absolute ethanol. Yield: 2.44 g (44%). ^{1}H NMR (500 MHz, $CDCl_3$): δ 8.39 (d, J = 7.6 Hz, 1H), 8.17 (dd, J = 6.3, 2.9 Hz, 1H), 8.00 (d, J = 8.7 Hz, 1H), 7.95 (d, J = 7.9 Hz, 1H), 7.72−7.64 (m, 2H), 7.58−7.52 (m, 2H). ^{13}C{^{1}H} NMR (126 MHz, $CDCl_3$): δ 182.6, 137.8, 137.4, 135.5, 134.1, 132.5, 132.0, 131.4, 131.1, 130.5, 129.1, 128.6, 126.8, 126.3, 126.1, 125.3, 122.1. Elem. Anal. Calcd for $C_{17}H_8Cl_2O$: C, 68.26; H, 2.70. Found: C, 68.33; H, 2.38. HRMS (MALDI-TOF, m/z): calcd for $C_{17}H_9Cl_2O^+$ [M+H$^+$], 299.0024; found, 299.0031. Mp: 188−189 °C. R_f (toluene/CH_2Cl_2, 10:1): 0.39.

*6,8-Dichloro-7-(2,6-dimethoxyphenyl)-7H-benzo[de]anthracen-7-ol (**3**).* To a dry 250 mL round-bottom flask equipped with a septum and evacuated under an Ar atmosphere were added dry diethyl ether (10 mL) and 1,3-dimethoxybenzene (580 mg, 4.20 mmol) followed by the dropwise addition of n-BuLi (2.5 M in hexane, 2.0 mL, 4.5 mmol). The mixture was stirred for 2 h at ambient temperature, whereupon the solution turned cloudy white. Compound **2** (500 mg, 1.67 mmol) was dissolved in a sufficient volume of dry benzene and added via syringe through the septum to the lithiated reagent. The solution became red immediately after addition. The mixture was then stirred at ambient temperature, and the reaction progression was followed by TLC analysis (tolene/CH_2Cl_2, 10:1). After 1 h, compound **2** was absent in the reaction mixture, and the reaction was quenched by the addition of 2-propanol. The solvents were removed by evaporation in vacuo. The residue was precipitated from a mixture of diethyl ether and heptane, and the off-white solid was filtered on a Büchner funnel. The crude material was suspended in water, and the mixture was stirred for 30 min, filtered on a Büchner funnel, and washed with water. The material was purified by column chromatography (toluene/CH_2Cl_2, 10:1). Yield: 200 mg (28%). ^{1}H NMR (500 MHz, $CDCl_3$): δ 8.36 (s, 1H), 8.27 (d, J = 7.6, 1H), 8.14 (dd, J = 7.9, 1.5 Hz, 1H), 7.78 (d, J = 8.1, 1H), 7.66 (d, J = 8.6 Hz, 1H), 7.55 (t, J = 7.8 Hz, 1H), 7.42 (d, J = 8.6 Hz, 1H), 7.30 (dd, J = 7.8, 1.5 Hz, 1H), 7.25 (t, J = 7.8 Hz, 1H, overlap with $CDCl_3$ peak), 7.14 (t, J = 8.3 Hz, 1H), 6.63 (d, J = 8.5 Hz, 1H), 6.24 (d, J = 8.2 Hz, 1H), 4.13 (s, 3H), 2.60 (s, 3H). ^{13}C{^{1}H} NMR (126 MHz, $CDCl_3$): δ 160.4, 156.9, 138.6, 137.5, 134.5, 133.5, 132.3, 131.8, 131.2, 130.5, 129.1, 128.8, 128.6, 128.3, 127.9, 127.7, 125.5, 121.2, 120.8, 120.4, 106.8, 104.3, 76.4, 56.3, 55.5. Elem. Anal. Calcd for $C_{25}H_{18}Cl_2O_3$: C, 68.66; H, 4.15; Found: C, 68.51; H, 4.05. HRMS (MALDI-TOF, m/z): calcd for $C_{25}H_{17}Cl_2O_2^+$ [M$^+$ − OH], 419.0600; found, 419.0599. Mp: >200 °C (degrad). R_f (toluene/CH_2Cl_2, 10:1): 0.21.

*6,8-Dichloro-7-(2,6-dimethoxyphenyl)benzo[de]anthracenium Tetrafluoroborate (**3a**).* Compound **3** (113 mg, 0.258 mmol) was dissolved in $CHCl_3$ (15 mL) and $HBF_{4(aq)}$ (50%, 2.0 mL, 0.26 mmol). The resulting mixture was stirred for 1 h at ambient temperatures resulting in a red colored solution. The organic solvent was removed by evaporation in vacou giving a brown solid, which was suspended in diethyl ether, stirred and red precipitate was filtered off, washed with diethyl ether, and dried. Yield: 120 mg (92%). ^{1}H NMR (500 MHz, DMSO-d_6): δ 9.11 (t, J = 7.6 Hz, 1H), 8.01 (d, J = 7.1 Hz, 1H), 7.95−7.86 (m, 2H), 7.80 (t, J = 7.9 Hz, 1H), 7.73 (d, J = 7.4 Hz, 1H), 7.36 (t, J = 8.4 Hz, 1H), 6.68 (d, J = 8.4 Hz, 2H), 6.41 (d, J = 9.6 Hz, 1H), 3.51 (s, 6H). ^{13}C{^{1}H} NMR (126 MHz, DMSO-d_6): δ 185.2(+), 157.7(+), 140.8(−), 139.4(+), 134.7(+), 133.5(+), 132.1(−), 130.7(−), 129.7(−), 129.5(−), 129.1(+), 129.0(−), 127.8(+), 127.8(+), 127.8(−), 126.4(−), 126.2(+), 125.6(+), 123.6(−), 117.9(+), 104.3(−), 55.6(−).

*Naphtho[8′,1′,2′:7,8,1]isochromeno[3,4,5,6-klmn]xanthenium Hexafluorophosphate (**4**).* In a 100 mL round-bottom flask were added **3** (40 mg, 0.091 mmol) and glacial acetic acid (20 mL). Upon stirring, the brown mixture turned gradually green. $HBr_{(aq)}$ (48%, 20 mL) was added to the mixture in one portion, and the reaction mixture gradually turned purple. The reaction was then heated to reflux for 48 h. The mixture was allowed to reach ambient temperature, and the reaction $KPF_{6(aq)}$ (0.2 M, 200 mL) was added upon stirring, and the finely divided precipitate was filtered off and washed with water. The crude material was dissolved in CH_2Cl_2, dried over $MgSO_4$, and filtered, and the solvent was removed by evaporation in vacuo. The red material was purified by column chromatography (CH_2Cl_2/CH_3OH, 20:1). Yield: 18 mg (42%). ^{1}H NMR (500 MHz, CD_2Cl_2): δ 9.28 (d, J = 8.1 Hz, 1H), 9.09 (d, J = 9.1 Hz, 1H), 8.77 (d, J = 8.0 Hz, 1H), 8.68 (d, J = 7.9 Hz, 1H), 8.47 (t, J = 8.4, 1H), 8.46 (t, J = 8.2 Hz, 1H) 8.36 (t, J = 7.9 Hz, 1H), 8.28 (d, J = 9.2 Hz, 1H), 8.04 (d, J = 8.6 Hz, 1H), 7.92 (d, J = 8.3 Hz, 1H), 7.87 (d, J = 8.4 Hz, 1H). ^{13}C{^{1}H} NMR (126 MHz, CD_3CN): δ 161.5(+), 156.3(+), 153.3(+), 152.9(+), 148.1(−), 142.8(+), 141.5(−), 141.1(−), 135.8(+), 135.5(−), 131.7(−), 131.1(−), 129.9(+), 128.2(+), 122.2(+), 120.8(−), 119.5(−), 116.8(−), 115.0(+), 113.6(−), 113.2(−), 110.6(+), 110.0(+). HRMS (MALDI-TOF, m/z): calcd for $C_{23}H_{11}O_2^+$ [M$^+$], 319.0754; found, 319.0752. Elem. Anal. Calcd for $C_{23}H_{11}F_6O_2P$: C, 59.50; H, 2.39. Found: C, 59.44; H, 2.36. R_f (CH_3OH/CH_2Cl_2, 1:20): 0.17.

*(2,6-Dimethoxyphenyl)(2-methoxynaphtalen-1-yl)methanone (**6**).* Thionyl chloride (8 mL, 110 mmol) and catalytic amounts of DMF were added to a suspension of 2,6-dimethoxybenzoic acid (8.01 g, 44 mmol) in dry toluene (60 mL). The solution was heated for 3 h at 65 °C under a nitrogen atmosphere. The mixture was allowed to reach ambient temperature, and excess thionyl chloride was removed by evaporation in vacuo, leaving a yellow oil. The oil was dissolved in dry CH_2Cl_2 (60 mL), and 2-methoxynaphthalene (6.60 g, 42 mmol) was added. The reaction mixture was cooled to 0 °C, while still under a nitrogen atmosphere. $AlCl_3$ (6.44 g, 48.3 mmol) was added in small portions, which resulted in a red colored solution. When the addition was completed, the solution was stirred at 0 °C for 2 h and then quenched by the addition of ice water (150 mL). The phases were separated, and the water phase was extracted with CH_2Cl_2 (3 × 50 mL). The combined organic phases were washed with $NaOH_{(aq)}$ (1 M, 3 × 75 mL) and brine (2 × 50 mL) and dried under a vacuum. The crude product was recrystallized from ethanol, giving white crystals. Yield: 8.92 g (63%). ^{1}H NMR (500 MHz, $CDCl_3$): δ 8.15 (dd, J = 8.6 Hz, 0.9 Hz, 1H), 7.85 (d, J = 9.0 Hz, 1H), 7.77 (d, J = 8.1

DOI: 10.1021/acs.joc.8b02978
J. Org. Chem. 2019, 84, 2556−2567

Hz, 1H), 7.48 (ddd, J = 8.6, 6.8, 1.3 Hz, 1H), 7.36 (ddd, J = 8.1, 6.8, 0.9 Hz, 1H), 7.27 (t, J = 8.4 Hz, 1H), 7.17 (d, J = 9.0 Hz, 1H), 6.55 (d, J = 8.4 Hz, 2H), 3.64 (s, 3H), 3.60 (s, 6H). $^{13}C\{^1H\}$ NMR (126 MHz, $CDCl_3$): δ 196.9(+), 158.5(+), 155.9(+), 132.0(−), 132.0(+), 131.1(−), 129.3(+), 127.9(−), 127.4(−), 127.0(+), 125.5(−), 124.1(−), 122.5(+), 114.4(−), 104.6(−), 57.4(−), 56.2(−). HRMS (MALDI-TOF, m/z): calcd for $C_{20}H_{19}O_4^+$ [M + H$^+$], 323.1278; found, 323.1280. Mp: 168−170 °C. R_f (2:1 heptane/ethyl acetate): 0.38. Elem. Anal. Calcd for $C_{20}H_{18}O_4$: C, 74.52; H, 5.63. Found: C, 74.14; H, 5.60.

*(2-Hydroxy-6-methoxyphenyl)(2-methoxynaphtalen-1-yl)-methanone (**7**).* The method reported by Torricelli et al. was followed.[53] In a three-neck flask fitted with a septum and a thermometer, compound **6** (8.71 g, 16.8 mmol) was dissolved in dry CH_2Cl_2 (250 mL) and the mixture cooled to −78 °C. A solution of BBr_3 (1 M in CH_2Cl_2, 27 mL, 27 mmol) was added dropwise, and the reaction mixture was stirred for 30 min at −78 °C, after which the cooling was removed. The reaction was allowed to reach ambient temperature and was stirred for 2.5 h. Hereafter, the reaction was quenched by the dropwise addition of ethanol (30 mL). The volatiles were removed by evaporation in vacuo. The crude product was dissolved in a minor volume of CH_2Cl_2 and filtered through a short pad of silica using CH_2Cl_2 as an eluent. The solvent was removed by evaporation in vacuo, yielding a yellow solid. The crude material was recrystallized from ethyl acetate, giving bright yellow crystals. Yield: 6.80 g (82%). ^1H NMR (500 MHz, DMSO-d_6): δ 12.20 (s, 1H), 8.01 (d, J = 9.1 Hz, 1H), 7.91 (dd, J = 8.0 Hz, 1.0 Hz, 1H), 7.52 (dd, J = 8.4 Hz, 1.1 Hz, 1H), 7.48 (d, J = 9.1 Hz, 1H), 7.44−7.39 (m, 2H), 7.36 (ddd, J = 8.0, 6.8, 1.1 Hz, 1H), 6.58 (dd, J = 8.4, 0.9 Hz, 1H), 6.44 (dd, J = 8.5, 0.9 Hz, 1H), 3.75 (s, 3H), 3.20 (s, 3H). $^{13}C\{^1H\}$ NMR (126 MHz, DMSO-d_6): δ 200.0(+), 161.9(+), 160.7(+), 153.0(+), 136.2(−), 130.5(−), 130.1(+), 128.2(+), 128.1(−), 127.0(−), 126.1(+), 123.7(−), 123.3(−), 114.2(+), 113.9(−), 109.7(−), 102.6(−), 56.6(−), 55.8(−). HRMS (MALDI-TOF, m/z): calcd for $C_{19}H_{17}O_4^+$ [M + H$^+$], 309.1121; found, 309.1123. Mp: 143−146 °C. R_f (2:1 heptane/EtOAc): 0.54. Elem. Anal. Calcd for $C_{19}H_{16}O_4$: C, 74.01; H, 5.23. Found: C, 73.77; H, 5.21.

*11-Methoxybenzo[a]xanthen-12-one (**8**).* The method reported by Torricelli et al. was followed.[53] Compound **7** (2.09 g, 6.78 mmol) was placed in a sealed container and heated to 225 °C, upon which it melted. After 5 h, TLC analysis (2:1 heptane/EtOAc) showed no trace of the starting material present and the heat was removed. After the mixture cooled to ambient temperature, the brown solid was dissolved in CH_2Cl_2 and filtered through a short pad of silica using CH_2Cl_2 as an eluent. The first eluting fraction contained an impurity, which was separated from the other fractions. The pure fractions were collected, and the solvent was removed in vacuo, giving an off-white powder. Yield: 1.19 g (64%). ^1H NMR (500 MHz, $CDCl_3$): δ 10.06 (d, J = 8.8 Hz, 1H), 8.09 (d, J = 9.0 Hz, 1H), 7.89 (dd, J = 8.7 Hz, 1.3 Hz, 1H), 7.74 (ddd, J = 8.8, 6.8, 1.3 Hz, 1H), 7.64−7.55 (m, 2H), 7.51 (d, J = 9.0 Hz, 1H), 7.13 (dd, J = 8.4, 0.9 Hz, 1H), 6.87 (d, J = 8.3 Hz, 1H), 4.08 (s, 3H). $^{13}C\{^1H\}$ NMR (126 MHz, $CDCl_3$): δ 196.9(+), 158.5(+), 155.9(+), 132.0(−), 132.0(+), 131.1(−), 129.3(+), 127.9(−), 127.4(−), 127.0(+), 125.5(−), 124.1(−), 122.5(+), 114.4(−), 104.6(−), 57.4(−), 56.2(−). HRMS (MALDI-TOF, m/z): calcd for $C_{18}H_{13}O_3^+$ [M + H$^+$], 277.0859; found, 277.0862. Mp: 198−201 °C. R_f (2:1 heptane/EtOAc): 0.35.

*11-Methoxy-12-(2-methoxyphenyl)-12H-benzo[a]xanthen-12-ol (**9**).* A suspension of lithium metal (100 mg, 14.4 mmol) in diethyl ether (10 mL) was placed in a dry three-necked flask equipped with a reflux condenser and an addition funnel. 2-Bromo-anisole (1.2 mL, 9.6 mmol) dissolved in diethyl ether (10 mL) was added to the refluxing solution over a period of 30 min. When the addition was complete, the mixture was stirred at gentle refluxing conditions for 3.5 h. The milky solution was added via a syringe to a suspension of **8** (1.0 g, 3.6 mmol) in benzene (50 mL) heated to 50 °C. The mixture was stirred for 30 min, whereupon water (20 mL) was added, generating an off-white precipitate. The volatiles were removed by evaporation in vacuo. The solid material was filtered on a Büchner funnel, washed with water, and dried on the filter. The white powder was dissolved in CH_2Cl_2 (200 mL), dried over Na_2SO_4, and filtered. Heptane (50 mL) was added, and CH_2Cl_2 was removed by evaporation in vacuo. The resulting white precipitate was filtered off and washed with heptane (3 × 50 mL). The white material cocrystallized with CH_2Cl_2. CH_2Cl_2 was removed by dissolving the material in hot toluene in a round-bottom flask. Toluene was removed by evaporation in vacuo, and the white powder was dried in vacuo (<1 mbar). Yield: 1.23 g (88%). ^1H NMR (500 MHz, CD_2Cl_2): δ 8.70−8.57 (m, 1H), 8.09 (d, J = 7.4 Hz, 1H), 7.75 (d, J = 8.9 Hz, 1H), 7.72−7.67 (m, 1H), 7.31 (d, J = 8.9 Hz, 1H), 7.29−7.19 (m, 3H), 7.13 (ddd, J = 8.0, 7.3, 1.8 Hz, 1H), 7.05 (td, J = 7.6, 1.3 Hz, 1H), 6.87 (dd, J = 8.3, 1.1 Hz, 1H), 6.64 (dd, J = 8.1, 1.2 Hz, 1H), 6.60 (dd, J = 8.2, 1.1 Hz, 1H), 5.37 (s, 1H), 3.69 (s, 3H), 3.26 (s, 3H). $^{13}C\{^1H\}$ NMR (126 MHz, CD_2Cl_2): δ 157.6(+), 157.1(+), 150.5(+), 148.4(+), 136.4(+), 131.9(+), 131.8(+), 130.5(−), 129.1(−), 128.9(−), 128.6(−), 127.6(−), 127.6(−), 126.1(−), 124.0(−), 119.8(−), 117.8(−), 116.8(+), 115.9(+), 113.2(−), 109.7(−), 106.5(−), 71.2(+), 56.4(−), 55.9(−). HRMS (MALDI-TOF, m/z): calcd for $C_{25}H_{19}O_3^+$ [M$^+$ − OH], 367.1329; found, 367.1326. Mp: >240 °C (degrad.). R_f (toluene/CH_2Cl_2, 10:1): 0.29.

*Benzo[a]chromeno[2,3,4-kl]xanthenium Hexafluorophosphate (**10**).* In a round-bottom flask, pyridine hydrochloride (8.4 g, 73 mmol) was heated to 190 °C until the material solidified on the inside of the flask. The material was melted into the flask using a heat gun, and **9** (420 mg, 1.1 mmol) was added in one portion upon stirring. The mixture was stirred for 5 min at 180−190 °C. The heating was removed, and the mixture was allowed to reach ambient temperature. The solid red material was dissolved in water (100 mL), and the solution was poured into an aqueous solution of $KPF_{6(aq)}$ (0.2 M, 400 mL) with vigorous stirring. The red solid was filtered off and dried by suction. The solid was suspended in CH_2Cl_2, stirred, and filtered. The organic phase was dried over $MgSO_4$ and filtered, and the solvent was removed by evaporation in vacuo. The red solid material was dissolved in a minor volume of acetonitrile and poured into diethyl ether (400 mL) with vigorous stirring. The resulting red precipitate was allowed to form, filtered off, and dried. Yield: 224 mg (44%). Note that the product precipitates with a trace of CH_3CN. ^1H NMR (500 MHz, CD_3CN): δ 8.73 (d, J = 9.1 Hz, 1H), 8.60 (d, J = 8.5 Hz, 1H), 8.49 (t, J = 8.4 Hz, 1H), 8.38 (dd, J = 8.5, 1.6 Hz, 1H), 8.23−8.18 (m, 1H), 8.15 (ddd, J = 8.6, 7.1, 1.6 Hz, 1H), 7.99−7.91 (m, 4H), 7.83 (ddd, J = 8.0, 7.0, 1.1 Hz, 1H), 7.68 (ddd, J = 8.4, 7.0, 1.4 Hz, 1H), 7.49 (ddd, J = 8.3, 7.1, 1.2 Hz, 1H). $^{13}C\{^1H\}$ NMR (126 MHz, CD_3 CN): δ 163.0(+), 158.3(+), 155.5(+), 152.6(+), 152.3(+), 146.2(−), 141.9(−), 141.3(−), 132.8(+), 131.6(−), 130.8(−), 130.4(−), 130.4(−), 130.2(+), 127.2(−), 126.6(−), 120.6(−), 119.0(+), 118.5(−), 116.1(+), 115.7(+), 112.9(−), 112.0(−). HRMS (MALDI-TOF, m/z): calcd for $C_{23}H_{13}O_2^+$ [M$^+$], 321.0910; found, 321.0919.

*3,7-Dimethyl-3,7-dihydrobenzo[a]quinolino[2,3,4-kl]acridinium Hexafluorophosphate (**11**).* Compound **10** (243 mg, 0.52 mmol) and benzoic acid (4.0 g, 33 mmol) were dissolved in *N*-methylpyrrolidone (4 mL) in a three-necked flask equipped with a stopper, a septum, and a reflux condenser fitted with a balloon on top. Methylamine (33% in absolute ethanol, 4 mL, 32 mmol) was added via a syringe through the septum. The mixture was heated on an oil bath adjusted to 90−95 °C for 18 h. The resulting green mixture was allowed to reach ambient temperature and poured into an acidified $KPF_{6(aq)}$ solution (0.2 M, acidified to pH 1−2 using 1 M $HCl_{(aq)}$, 400 mL) with vigorous stirring. The green precipitate was filtered off, washed with water (3 × 25 mL), and dried on a Büchner funnel. The material was washed with diethyl ether (3 × 100 mL) and then dissolved in CH_2Cl_2, dried over Na_2SO_4, and filtered. The volume was reduced to a minimum by evaporation in vacuo and poured into diethyl ether (400 mL) with vigorous stirring. The blue-green precipitate was allowed to settle and filtered off. The material was purified by column chromatography (acetone/CH_2Cl_2, 10:90, dry loading on Celite). The blue solid was dissolved in a minor volume of CH_2Cl_2, filtered, and reprecipitated from diethyl ether. Yield: 30 mg (12%). ^1H NMR (500 MHz, CD_3 CN): δ 8.44 (d, J = 9.4 Hz, 1H), 8.27 (t, J = 8.5 Hz, 1H), 8.14 (d, J = 8.5 Hz, 1H), 8.09−8.02 (m, 2H),

DOI: 10.1021/acs.joc.8b02978
J. Org. Chem. 2019, 84, 2556−2567

8.01−7.96 (m, 1H), 7.96−7.88 (m, 2H), 7.66−7.59 (m, 3H), 7.38 (ddd, J = 8.5, 7.0, 1.4 Hz, 1H), 7.22 (ddd, J = 8.2, 6.8, 1.1 Hz, 1H), 4.25 (s, 3H), 4.17 (s, 3H). $^{13}C\{^1H\}$ NMR (126 MHz, CD_3CN): δ 146.1(+), 144.9(+), 143.0(+), 140.6(+), 140.4(+), 139.5(−), 137.1(−), 136.7(−), 131.7(−), 131.1(+), 131.1(+), 129.7(−), 128.8(−), 128.6(−), 125.9(−), 123.9(−), 120.9(+), 120.6(+), 118.5(−), 116.1(−), 115.7(+), 107.1(−), 106.9(−), 38.7(−), 37.7(−). HRMS (MALDI-TOF, m/z): calcd for $C_{25}H_{19}N_2^+$ [M^+], 347.1543; found, 347.1552. Elem. Anal. Calcd for $C_{25}H_{19}F_6N_2P$: C, 60.98; H, 3.89; N, 5.69. Found: C, 60.95; H, 3.84; N, 5.58. R_f (CH_2Cl_2/acetone, 10:90): 0.17.

*12-(2,6-Dimethoxyphenyl)-11-methoxybenzo[a]xanthenium Hexafluorophosphate (**12**).* A dry round-bottom flask equipped with a septum was evacuated under an Ar atmosphere, and 1,3-dimethoxybenzene (0.7 mL, 5.32 mmol) dry diethyl ether (10 mL), benzene (10 mL), and TMEDA (0.75 mL, 5.01 mmol) were added. The mixture was cooled to 0 °C, and then *n*-BuLi (2.5 M in hexane, 2 mL, 5 mmol) was added. The cooling was removed, and the mixture was stirred for 3 h. A solution of **8** (0.805 g, 2.91 mmol) in dry benzene (60 mL) was added via a syringe. After 18 h at ambient temperature, TLC analysis still showed the presence of the starting material, and a new portion of lithiated 1,3-methoxybenzene was prepared following the above procedure. The reaction mixture was added to the new lithium species al cannula. After 2 h, the flask was fitted with a condenser, and the reaction mixture was heated to 55 °C for 48 h and then quenched by the addition of water (50 mL) and aqueous KOH (2 M, 50 mL). The volatiles were removed by evaporation in vacuo, leaving a sticky yellow residue. The residue was dissolved in CH_2Cl_2 (8 mL), and the product precipitated by the addition of heptane (500 mL). The yellow precipitate was filtered off and washed with heptane. The crude product was dissolved in a mixture of methanol (100 mL) and acetonitrile (60 mL) upon heating to 55 °C. The mixture was allowed to reach ambient temperature, and upon stirring, $HCl_{(aq)}$ (6 M, 20 mL) was added followed by $KPF_{6(aq)}$ (0.2 M, 150 mL), resulting in precipitation of a red powder. The product was filtered off and washed with water (2 × 100 mL) and diethyl ether (2 × 100 mL). The product was dissolved in a minor volume of acetonitrile and precipitated by the addition of excess diethyl ether. The product was filtered off and dried in vacuo (<1 mbar). Yield: 738 mg (47%). ^1H NMR (500 MHz, CD_3 CN): δ 8.85 (d, J = 9.2 Hz, 1H), 8.37 (t, J = 8.4 Hz, 1H), 8.23 (dd, J = 7.8, 1.5 Hz, 1H), 8.12 (d, J = 9.2 Hz, 1H), 7.86 (dd, J = 8.4, 0.7 Hz, 1H), 7.84−7.78 (m, 2H), 7.73 (t, J = 8.5 Hz, 1H), 7.55 (ddd, J = 8.8, 7.2, 1.5 Hz, 1H), 7.29 (dd, J = 8.2 Hz, 0.7 Hz, 1H), 6.95 (d, J = 8.5 Hz, 2H), 3.68 (s, 3H), 3.53 (s, 6H). $^{13}C\{^1H\}$ NMR (126 MHz, CD_3CN): δ 168.8(+), 162.9(+), 161.8(+), 156.6(+), 156.4(+), 149.7(−), 144.1(−), 134.0(−), 132.8(−), 132.7(+), 132.5(−), 130.7(+), 130.5(−), 127.0(−), 123.2(+), 119.1(−), 118.8(+), 117.06(+), 111.3(−), 110.3(−), 106.3(−), 58.4(−), 57.0(−). ^{19}F NMR (470 MHz, CD_3CN): δ −70.95 (d, J = 707.0 Hz). HRMS (MALDI-TOF, m/z): calcd for $C_{26}H_{21}O_4^+$ [M^+], 397.1434; found, 397.1445. Mp: >251 °C (decomp). R_f (9:1 CH_2Cl_2/acetone): 0.29. Elem. Anal. Calcd for $C_{26}H_{21}F_6O_4P$: C, 57.57; H, 3.90. Found: C, 57.63; H, 3.73.

*11-Methoxy-3,7-dimethyl-3,7-dihydrobenzo[a]quinolino[2,3,4-kl]acridinium Hexafluorophosphate (**13**).* Compound **12** (254 mg, 0.468 mmol) and benzoic acid (4.0 g, 33 mmol) were dissolved in *N*-methyl-pyrrolidone (4 mL) in a three-necked flask equipped with a stopper, a septum, and a reflux condenser fitted with a balloon on top. Methylamine (33% in absolute ethanol, 4 mL, 32 mmol) was added via a syringe through the septum. The mixture was heated on an oil bath adjusted to 90−95 °C for 18 h. The resulting green mixture was allowed to reach ambient temperature and poured into an acidified $KPF_{6(aq)}$ solution (0.2 M, acidified to pH 1−2 using 1 M $HCl_{(aq)}$, 400 mL) upon vigorous stirring. The green precipitate was filtered off, washed with water (3 × 25 mL), and dried by suction. The material was washed with diethyl ether (3 × 100 mL) and dried by suction. The material was dissolved in CH_2Cl_2, dried over Na_2SO_4, and filtered. The volume of the organic phase was reduced to a minimum by evaporation in vacuo and poured into diethyl ether (400 mL) upon vigorous stirring. The blue-green precipitate was allowed to settle and filtered off. The material was purified by column chromatography (acetone/CH_2Cl_2, 10:90, dry loading on Celite). The blue-green solid was dissolved in a minor volume of CH_2Cl_2, filtered, and reprecipitated from diethyl ether. Yield: 30 mg (12%). ^1H NMR (500 MHz, CD_3CN): δ 8.39 (d, J = 9.5 Hz, 1H), 8.23 (t, J = 8.5 Hz, 1H), 8.07−8.00 (m, 2H), 7.98 (d, J = 8.5, 1H), 7.91 (dd, J = 8.8, 8.1 Hz, 1H), 7.66 (d, J = 8.4 Hz, 1H), 7.61 (ddd, J = 8.0, 7.0, 1.1 Hz, 1H), 7.57 (d, J = 8.4 Hz, 1H), 7.52 (dd, J = 8.8, 0.8 Hz, 1H), 7.38 (ddd, J = 8.5, 7.0, 1.4 Hz, 1H), 6.76 (d, J = 8.0 Hz, 1H), 4.29 (s, 3H), 4.11 (s, 3H), 2.95 (s, 3H). $^{13}C\{^1H\}$ NMR (126 MHz, CD_3CN): δ 158.4(+), 144.5(+), 143.4(+), 142.5(+), 140.3(+), 139.9(+), 139.3(−), 137.8(−), 136.4(−), 132.6(+), 129.7(−), 129.3(+), 129.1(−), 128.6(−), 122.4(−), 121.4(+), 118.6(+), 116.0(−), 113.2(+), 109.8(−), 107.0(−), 106.9(−), 105.7(−), 55.7(−), 38.8(−), 38.1(−). HRMS (MALDI-TOF, m/z): calcd for $C_{26}H_{21}N_2O^+$ [M^+], 377.1648; found, 377.1658. Mp: >310 °C (decomp). R_f (CH_2Cl_2/acetone): 0.20.

*7,11-Dimethyl-7,11-dihydronaphtho[8′,1′,2′:7,8,1]isoquinolino-[3,4,5,6-klmn]acridinium Hexafluorophosphate (**14**).* From **11**, phosphorus pentoxide (3.7 g, 26 mmol) was added in small portions in phosphoric acid (85%, 2 mL, 39 mmol) placed in a round-bottom flask at ambient temperature. The mixture was stirred and heated on an oil bath set to 110 °C under a N_2 atmosphere for 1 h. The nitrogen flow was removed, and compound **11** (27 mg, 0.055 mmol) was added in one portion, and the mixture was stirred at 110 °C for 30 h in the open flask. The green mixture was allowed to reach ambient temperature and poured into $KPF_{6(aq)}$ (0.2 M, 200 mL). The green precipitate was filtered off and washed with $KPF_{6(aq)}$ solution (0.2 M, 2 × 100 mL) and then with water (3 × 50 mL). The solid was washed with dichloromethane (50 mL) and with methanol (50 mL) and dried. The solid was dissolved in acetonitrile through the filter, and the volume was reduced to a minimum in a vacuum. The solution was poured into diethyl ether upon stirring (250 mL). The finely divided green precipitate was allowed to form and was subsequently filtered off and dried. Yield: 9 mg (33%). From **12**, the same procedure as described for **11** was used with the difference that the reaction was stopped after 1 h. Compound **12** (30 mg, 0.057 mmol). Yield: 10 mg (36%). ^1H NMR (500 MHz, CD_3CN): δ 8.06−7.98 (m, 2H), 7.96 (d, J = 9.4 Hz, 1H), 7.77 (d, J = 7.5 Hz, 1H), 7.57 (t, J = 8.0 Hz, 1H), 7.54−7.48 (m, 2H), 7.41 (d, J = 9.3 Hz, 1H), 7.23 (d, J = 8.5 Hz, 1H), 7.08 (d, J = 8.3 Hz, 1H), 7.04 (d, J = 8.3 Hz, 1H), 3.75 (s, 3H), 3.37 (s, 3H). $^{13}C\{^1H\}$ NMR (126 MHz, CD_3CN): δ 142.4(+), 141.7(+), 141.2(+), 140.3(−), 139.1(+), 137.4(−), 136.9(+), 135.7(−), 133.3(+), 131.8(−), 128.8(−), 128.0(+), 127.2(+), 126.7(−), 122.0(+), 116.4(−), 116.2(−), 116.0(+), 115.3(+), 112.9(−), 110.2(+), 107.5(−), 107.1(−), 37.7(−), 35.9(−). HRMS (MALDI-TOF, m/z): calcd for $C_{25}H_{17}N_2^+$ [M^+], 345.1386; found, 345.1395.

*11-Hydroxybenzo[a]chromeno[2,3,4-k,l]xanthenium Hexafluorophosphate (**15**).* In a 100 mL round-bottom flask fitted with a condenser, **12** (198 mg, 0.499 mmol) was dissolved in acetic acid (20 mL). $HBr_{(aq)}$ was added (48%, 10 mL), and the solution heated to refluxing conditions for 36 h. The heating was removed, and the reaction mixture was allowed to reach ambient temperature and then poured into 0.2 M $KPF_{6(aq)}$ (0.2 M, 100 mL). The precipitate was filtered off and washed with water and then with heptane. The material was purified by column chromatography (9:1 CH_2Cl_2/acetone). Yield: 12 mg (7%) ^1H NMR (500 MHz, CD_3CN): δ 8.38 (d, J = 9.0 Hz, 1H), 8.18 (d, J = 8.4 Hz, 1H), 8.06−7.99 (m, 2H), 7.69 (d, J = 9.0 Hz, 1H), 7.66−7.61 (m, 1H), 7.60−7.51 (m, 3H), 7.49 (d, J = 8.2 Hz, 1H), 6.64 (d, J = 7.7 Hz, 1H), 6.24 (d, J = 8.8 Hz, 1H). ^{19}F NMR (470 MHz, CD_3CN): δ −70.97 (d, J = 705.6 Hz). HRMS (MALDI-TOF, m/z): calcd for [$C_{23}H_{13}O_3^+$], 337.0859; found, 337.0859. Mp: >170 °C (decomp). R_f (9:1 CH_2Cl_2/acetone): 0.31. Due to the poor solubility of the material, ^{13}C NMR could not be obtained.

DOI: 10.1021/acs.joc.8b02978
J. Org. Chem. 2019, 84, 2556−2567

■ ASSOCIATED CONTENT

Supporting Information

The Supporting Information is available free of charge on the ACS Publications website at DOI: 10.1021/acs.joc.8b02978.

NMR spectra for all new compounds, cyclic voltammograms, absorption, emission, and excitation spectra, Cartesian coordinates from DFT optimized structures, and calculated vertical excitation energies and orbital plots (PDF)

■ AUTHOR INFORMATION

Corresponding Author

*E-mail: bwl@nano.ku.dk.

ORCID

Sidsel A. Bogh: 0000-0001-9827-6205

Ole Hammerich: 0000-0002-2080-1206

Bo W. Laursen: 0000-0002-1120-3191

Author Contributions

†M.R. and M.S. contributed equally.

Notes

The authors declare the following competing financial interest(s): Bo W. Laursen is associated with the company KU-dyes, which produces and sells fluorescent dyes (including triangulenium dyes).

■ ACKNOWLEDGMENTS

The work was supported by the Danish Council of Independent Research (DFF-6111-00483, DFF-1337-00005, and DFF-1335-00773).

■ REFERENCES

(1) Johnson, I. *The Molecular Probes Handbook: A Guide to Fluorescent Probes and Labeling Technologies*, 11th ed.; Life Technologies Corporation, 2010.

(2) Shieh, P.; Dien, V. T.; Beahm, B. J.; Castellano, J. M.; Wyss-Coray, T.; Bertozzi, C. R. CalFluors: A Universal Motif for Fluorogenic Azide Probes across the Visible Spectrum. *J. Am. Chem. Soc.* **2015**, *137* (22), 7145−7151.

(3) Lukinavičius, G.; Reymond, L.; Umezawa, K.; Sallin, O.; D'Este, E.; Göttfert, F.; Ta, H.; Hell, S. W.; Urano, Y.; Johnsson, K. Fluorogenic Probes for Multicolor Imaging in Living Cells. *J. Am. Chem. Soc.* **2016**, *138* (30), 9365−9368.

(4) Lukinavičius, G.; Reymond, L.; D'Este, E.; Masharina, A.; Göttfert, F.; Ta, H.; Güther, A.; Fournier, M.; Rizzo, S.; Waldmann, H.; Blaukopf, C.; Sommer, C.; Gerlich, D. W.; Arndt, H.-D.; Hell, S. W.; Johnsson, K. Fluorogenic probes for live-cell imaging of the cytoskeleton. *Nat. Methods* **2014**, *11*, 731−733.

(5) Lukinavičius, G.; Blaukopf, C.; Pershagen, E.; Schena, A.; Reymond, L.; Derivery, E.; Gonzalez-Gaitan, M.; D'Este, E.; Hell, S. W.; Wolfram Gerlich, D.; Johnsson, K. SiR−Hoechst is a far-red DNA stain for live-cell nanoscopy. *Nat. Commun.* **2015**, *6*, 8497.

(6) Kushida, Y.; Nagano, T.; Hanaoka, K. Silicon-substituted xanthene dyes and their applications in bioimaging. *Analyst* **2015**, *140* (3), 685−695.

(7) Ikeno, T.; Nagano, T.; Hanaoka, K. Silicon-substituted Xanthene Dyes and Their Unique Photophysical Properties for Fluorescent Probes. *Chem. - Asian J.* **2017**, *12* (13), 1435−1446.

(8) Huang, Y.-L.; Walker, A. S.; Miller, E. W. A Photostable Silicon Rhodamine Platform for Optical Voltage Sensing. *J. Am. Chem. Soc.* **2015**, *137* (33), 10767−10776.

(9) Hirabayashi, K.; Hanaoka, K.; Takayanagi, T.; Toki, Y.; Egawa, T.; Kamiya, M.; Komatsu, T.; Ueno, T.; Terai, T.; Yoshida, K.; Uchiyama, M.; Nagano, T.; Urano, Y. Analysis of Chemical Equilibrium of Silicon-Substituted Fluorescein and Its Application to Develop a Scaffold for Red Fluorescent Probes. *Anal. Chem.* **2015**, *87* (17), 9061−9069.

(10) Hanaoka, K.; Urano, Y. Development of Silicon-substituted Xanthene Dyes and Their Application to Fluorescent Probes. *Yuki Gosei Kagaku Kyokaishi* **2016**, *74* (5), 512−520.

(11) Grimm, J. B.; Klein, T.; Kopek, B. G.; Shtengel, G.; Hess, H. F.; Sauer, M.; Lavis, L. D. Synthesis of a Far-Red Photoactivatable Silicon-Containing Rhodamine for Super-Resolution Microscopy. *Angew. Chem., Int. Ed.* **2016**, *55* (5), 1723−1727.

(12) Grimm, J. B.; English, B. P.; Chen, J.; Slaughter, J. P.; Zhang, Z.; Revyakin, A.; Patel, R.; Macklin, J. J.; Normanno, D.; Singer, R. H.; Lionnet, T.; Lavis, L. D. A general method to improve fluorophores for live-cell and single-molecule microscopy. *Nat. Methods* **2015**, *12* (3), 244−250.

(13) Grimm, J. B.; Brown, T. A.; Tkachuk, A. N.; Lavis, L. D. General Synthetic Method for Si-Fluoresceins and Si-Rhodamines. *ACS Cent. Sci.* **2017**, *3* (9), 975−985.

(14) Erdmann, R. S.; Takakura, H.; Thompson, A. D.; Rivera-Molina, F.; Allgeyer, E. S.; Bewersdorf, J.; Toomre, D.; Schepartz, A. Super resolution imaging of the Golgi in live cells with a bioorthogonal ceramide probe. *Angew. Chem., Int. Ed.* **2014**, *53*, 10242−10246.

(15) Butkevich, A. N.; Mitronova, G. Y.; Sidenstein, S. C.; Klocke, J. L.; Kamin, D.; Meineke, D. N. H.; D'Este, E.; Kraemer, P. T.; Danzl, J. G.; Belov, V. N.; Hell, S. W. Fluorescent Rhodamines and Fluorogenic Carbopyronines for Super Resolution STED Microscopy in Living Cells. *Angew. Chem., Int. Ed.* **2016**, *55* (10), 3290−3294.

(16) Butkevich, A. N.; Belov, V. N.; Kolmakov, K.; Sokolov, V. V.; Shojaei, H.; Sidenstein, S. C.; Kamin, D.; Matthias, J.; Vlijm, R.; Engelhardt, J.; Hell, S. W. Hydroxylated fluorescent dyes for live cell labeling: synthesis, spectra and superresolution STED microscopy. *Chem. - Eur. J.* **2017**, *23* (50), 12114−12119.

(17) Zhou, X.; Lai, R.; Beck, J. R.; Li, H.; Stains, C. I. Nebraska Red: a phosphinate-based near-infrared fluorophore scaffold for chemical biology applications. *Chem. Commun.* **2016**, *52* (83), 12290−12293.

(18) Ogasawara, H.; Grzybowski, M.; Hosokawa, R.; Sato, Y.; Taki, M.; Yamaguchi, S. A far-red fluorescent probe based on a phosphafluorescein scaffold for cytosolic calcium imaging. *Chem. Commun.* **2018**, *54* (3), 299−302.

(19) Grzybowski, M.; Taki, M.; Yamaguchi, S. Selective Conversion of P = O-Bridged Rhodamines into P = O-Rhodols: Solvatochromic Near-Infrared Fluorophores. *Chem. - Eur. J.* **2017**, *23* (53), 13028−13032.

(20) Chai, X.; Cui, X.; Wang, B.; Yang, F.; Cai, Y.; Wu, Q.; Wang, T. Near-Infrared Phosphorus-Substituted Rhodamine with Emission Wavelength above 700 nm for Bioimaging. *Chem. - Eur. J.* **2015**, *21* (47), 16754−16758.

(21) Liu, J.; Sun, Y.-Q.; Zhang, H.; Shi, H.; Shi, Y.; Guo, W. Sulfone-Rhodamines: A New Class of Near-Infrared Fluorescent Dyes for Bioimaging. *ACS Appl. Mater. Interfaces* **2016**, *8* (35), 22953−22962.

(22) Grimm, J. B.; Gruber, T. D.; Ortiz, G.; Brown, T. A.; Lavis, L. D. Virginia Orange: A Versatile, Red-Shifted Fluorescein Scaffold for Single- and Dual-Input Fluorogenic Probes. *Bioconjugate Chem.* **2016**, *27* (2), 474−480.

(23) Grimm, J. B.; Sung, A. J.; Legant, W. R.; Hulamm, P.; Matlosz, S. M.; Betzig, E.; Lavis, L. D. Carbofluoresceins and Carborhodamines as Scaffolds for High-Contrast Fluorogenic Probes. *ACS Chem. Biol.* **2013**, *8* (6), 1303−1310.

(24) Kolmakov, K.; Belov, V. N.; Wurm, C. A.; Harke, B.; Leutenegger, M.; Eggeling, C.; Hell, S. W. A Versatile Route to Red-Emitting Carbopyronine Dyes for Optical Microscopy and Nanoscopy. *Eur. J. Org. Chem.* **2010**, *2010* (19), 3593−3610.

(25) Kolmakov, K.; Wurm, C.; Sednev, M. V.; Bossi, M. L.; Belov, V. N.; Hell, S. W. Masked red-emitting carbopyronine dyes with photosensitive 2-diazo-1-indanone caging group. *Photochem. Photobiol. Sci.* **2012**, *11* (3), 522−532.

(26) Sednev, M. V.; Wurm, C. A.; Belov, V. N.; Hell, S. W. Carborhodol: A New Hybrid Fluorophore Obtained by Combination

DOI: 10.1021/acs.joc.8b02978
J. Org. Chem. 2019, 84, 2556−2567

of Fluorescein and Carbopyronine Dye Cores. *Bioconjugate Chem.* **2013**, *24* (4), 690−700.
(27) Lavis, L. D. Teaching Old Dyes New Tricks: Biological Probes Built from Fluoresceins and Rhodamines. *Annu. Rev. Biochem.* **2017**, *86* (1), 825−843.
(28) Grimm, J. B.; Muthusamy, A. K.; Liang, Y.; Brown, T. A.; Lemon, W. C.; Patel, R.; Lu, R.; Macklin, J. J.; Keller, P. J.; Ji, N.; Lavis, L. D. A general method to fine-tune fluorophores for live-cell and in vivo imaging. *Nat. Methods* **2017**, *14* (10), 987−994.
(29) Meyer-Almes, F.-J. Fluorescence lifetime based bioassays. *Methods Appl. Fluoresc.* **2017**, *5*, 042002.
(30) Shivalingam, A.; Izquierdo, M. A.; Marois, A. L.; Vysniauskas, A.; Suhling, K.; Kuimova, M. K.; Vilar, R. The interactions between a small molecule and G-quadruplexes are visualized by fluorescence lifetime imaging microscopy. *Nat. Commun.* **2015**, *6*, 8178.
(31) Rich, R. M.; Stankowska, D. L.; Maliwal, B. P.; Sørensen, T. J.; Laursen, B. W.; Krishnamoorthy, R. R.; Gryczynski, Z.; Borejdo, J.; Gryczynski, I.; Fudala, R. Elimination of autofluorescence background from fluorescence tissue images by use of time-gated detection and the AzaDiOxaTriAngulenium (ADOTA) fluorophore. *Anal. Bioanal. Chem.* **2013**, *405* (6), 2065−2075.
(32) Hall, M. D.; Yasgar, A.; Peryea, T.; Braisted, J. C.; Jadhav, A.; Simeonov, A.; Coussens, N. P. Fluorescence polarization assays in high-throughput screening and drug discovery: a review. *Methods Appl. Fluoresc.* **2016**, *4* (2), 022001.
(33) Wawrzinek, R.; Ziomkowska, J.; Heuveling, J.; Mertens, M.; Herrmann, A.; Schneider, E.; Wessig, P. DBD Dyes as Fluorescence Lifetime Probes to Study Conformational Changes in Proteins. *Chem. - Eur. J.* **2013**, *19* (51), 17349−17357.
(34) Laursen, B. W.; Krebs, F. C. Synthesis, structure, and properties of azatriangulenium salts. *Chem. - Eur. J.* **2001**, *7* (8), 1773−1783.
(35) Bosson, J.; Gouin, J.; Lacour, J. Cationic triangulenes and helicenes: synthesis, chemical stability, optical properties and extended applications of these unusual dyes. *Chem. Soc. Rev.* **2014**, *43* (8), 2824−40.
(36) Bogh, S. A.; Simmermacher, M.; Westberg, M.; Bregnhøj, M.; Rosenberg, M.; De Vico, L.; Veiga, M.; Laursen, B. W.; Ogilby, P. R.; Sauer, S. P. A.; Sørensen, T. J. Azadioxatriangulenium and Diazaoxatriangulenium: Quantum Yields and Fundamental Photophysical Properties. *ACS Omega* **2017**, *2* (1), 193−203.
(37) Maliwal, B. P.; Fudala, R.; Raut, S.; Kokate, R.; Sørensen, T. J.; Laursen, B. W.; Gryczynski, Z.; Gryczynski, I. Long-Lived Bright Red Emitting Azaoxa-Triangulenium Fluorophores. *PLoS One* **2013**, *8* (5), No. e63043.
(38) Sørensen, T. J.; Laursen, B. W.; Luchowski, R.; Shtoyko, T.; Akopova, I.; Gryczynski, Z.; Gryczynski, I. Enhanced fluorescence emission of Me-ADOTA(+) by self-assembled silver nanoparticles on a gold film. *Chem. Phys. Lett.* **2009**, *476* (1−3), 46−50.
(39) Bogh, S. A.; Bora, I.; Rosenberg, M.; Thyrhaug, E.; Laursen, B. W.; Sørensen, T. J. Azadioxatriangulenium: exploring the effect of a 20 ns fluorescence lifetime in fluorescence anisotropy measurements. *Methods Appl. Fluoresc.* **2015**, *3* (4), 045001.
(40) Chib, R.; Mummert, M.; Bora, I.; Laursen, B. W.; Shah, S.; Pendry, R.; Gryczynski, I.; Borejdo, J.; Gryczynski, Z.; Fudala, R. Fluorescent biosensor for the detection of hyaluronidase: intensity-based ratiometric sensing and fluorescence lifetime-based sensing using a long lifetime azadioxatriangulenium (ADOTA) fluorophore. *Anal. Bioanal. Chem.* **2016**, *408* (14), 3811−3821.
(41) Sørensen, T. J.; Thyrhaug, E.; Szabelski, M.; Luchowski, R.; Gryczynski, I.; Gryczynski, Z.; Laursen, B. W. Azadioxatriangulenium: a long fluorescence lifetime fluorophore for large biomolecule binding assay. *Methods Appl. Fluoresc.* **2013**, *1* (2), 025001.
(42) Stewart, H. L.; Yip, P.; Rosenberg, M.; Sørensen, T. J.; Laursen, B. W.; Knight, A. E.; Birch, D. J. S. Nanoparticle metrology of silica colloids and super-resolution studies using the ADOTA fluorophore. *Meas. Sci. Technol.* **2016**, *27*, 045007.
(43) Rosenberg, M.; Rostgaard, K. R.; Liao, Z.; Madsen, A. O.; Martinez, K. L.; Vosch, T.; Laursen, B. W. Design, synthesis, and time-gated cell imaging of carbon-bridged triangulenium dyes with long fluorescence lifetime and red emission. *Chem. Sci.* **2018**, *9* (12), 3122−3130.
(44) Nicolas, C.; Bernardinelli, G.; Lacour, J. On the synthesis and optical properties of sulfur-bridged analogues of triangulenium cations and their precursors. *J. Phys. Org. Chem.* **2010**, *23* (11), 1049−1056.
(45) Macleod, L. C.; Allen, F. H. Benzanthrone [7-Benz[de]-anthracene-7-one]. *Org. Synth.* **1934**, *14*, 4.
(46) Gerasimenko, Y. E.; Sokolyuk, N. T.; Pisulina, L. P. Synthesis and Photochemical Characteristics of the Phenoxy Derivatives of Benzanthrone. *Zh. Org. Khim.* **1986**, *22* (3), 632−636.
(47) House, H. O.; Ghali, N. I.; Haack, J. L.; VanDerveer, D. Reactions of the 1,8-diphenylanthracene system. *J. Org. Chem.* **1980**, *45* (10), 1807−1817.
(48) For the addition of *ortho*-lithiated 1,3-dimethoxybenzene to sterically hinder ketones, benzene solutions are often found to be advantageous;[50] however, dried toluene will probably serve as a replacement.[71]
(49) Bora, I.; Bogh, S. A.; Rosenberg, M.; Santella, M.; Sørensen, T. J.; Laursen, B. W. Diazaoxatriangulenium: synthesis of reactive derivatives and conjugation to bovine serum albumin. *Org. Biomol. Chem.* **2016**, *14* (3), 1091−1101.
(50) Martin, J. C.; Smith, R. G. Factors Influencing the Basicities of Triarylcarbinols. The Synthesis of Sesquixanthydrol. *J. Am. Chem. Soc.* **1964**, *86* (11), 2252−2256.
(51) Bosson, J.; Labrador, G. M.; Pascal, S.; Miannay, F. A.; Yushchenko, O.; Li, H. D.; Bouffier, L.; Sojic, N.; Tovar, R. C.; Muller, G.; Jacquemin, D.; Laurent, A. D.; Le Guennic, B.; Vauthey, E.; Lacour, J. Physicochemical and Electronic Properties of Cationic 6 Helicenes: from Chemical and Electrochemical Stabilities to Far-Red (Polarized) Luminescence. *Chem. - Eur. J.* **2016**, *22* (51), 18394−18403.
(52) Torricelli, F.; Bosson, J.; Besnard, C.; Chekini, M.; Burgi, T.; Lacour, J. Modular synthesis, orthogonal post-functionalization, absorption, and chiroptical properties of cationic [6]helicenes. *Angew. Chem., Int. Ed.* **2013**, *52* (6), 1796−800.
(53) Grzybowski, M.; Skonieczny, K.; Butenschön, H.; Gryko, D. T. Comparison of Oxidative Aromatic Coupling and the Scholl Reaction. *Angew. Chem., Int. Ed.* **2013**, *52* (38), 9900−9930.
(54) Pieters, G.; Gaucher, A.; Prim, D.; Besson, T.; Giner Planas, J.; Teixidor, F.; Vinas, C.; Light, M. E.; Hursthouse, M. B. Binaphthyl platform as starting materials for the preparation of electron rich benzo[g,h,i]perylenes. Application to molecular architectures based on amino benzo[g,h,i]perylenes and carborane combinations. *Chem. Commun.* **2011**, *47* (27), 7725−7727.
(55) Suenaga, M.; Miyahara, Y.; Shimizu, N.; Inazu, T. Synthesis of the Trinaphthophenalenium Cation. *Angew. Chem., Int. Ed.* **1998**, *37* (1−2), 90−91.
(56) Bosson, J.; Gouin, J.; Lacour, J. Cationic triangulenes and helicenes: synthesis, chemical stability, optical properties and extended applications of these unusual dyes. *Chem. Soc. Rev.* **2014**, *43* (8), 2824−40.
(57) Dileesh, S.; Gopidas, K. R. Photoinduced electron transfer in azatriangulenium salts. *J. Photochem. Photobiol., A* **2004**, *162* (1), 115−120.
(58) Petersen, J. F.; Frederickson, C. K.; Marshall, J. L.; Rudebusch, G. E.; Zakharov, L. N.; Hammerich, O.; Haley, M. M.; Nielsen, M. B. Expanded Indacene−Tetrathiafulvalene Scaffolds: Structural Implications for Redox Properties and Association Behavior. *Chem. - Eur. J.* **2017**, *23* (53), 13120−13130.
(59) Christensen, M. A.; Rudebusch, G. E.; Parker, C. R.; Andersen, C. L.; Kadziola, A.; Haley, M. M.; Hammerich, O.; Nielsen, M. B. Diindenothienoacene−tetrathiafulvalene redox systems. *RSC Adv.* **2015**, *5* (61), 49748−49751.
(60) Christensen, M. A.; Parker, C. R.; Sørensen, T. J.; de Graaf, S.; Morsing, T. J.; Brock-Nannestad, T.; Bendix, J.; Haley, M. M.; Rapta, P.; Danilov, A.; Kubatkin, S.; Hammerich, O.; Nielsen, M. B. Mixed valence radical cations and intermolecular complexes derived from indenofluorene-extended tetrathiafulvalenes. *J. Mater. Chem. C* **2014**, *2* (48), 10428−10438.

DOI: 10.1021/acs.joc.8b02978
J. Org. Chem. 2019, 84, 2556−2567

(61) Adam, C.; Wallabregue, A.; Li, H. D.; Gouin, J.; Vanel, R.; Grass, S.; Bosson, J.; Bouffier, L.; Lacour, J.; Sojic, N. Electrogenerated Chemiluminescence of Cationic Triangulene Dyes: Crucial Influence of the Core Heteroatoms. *Chem. - Eur. J.* **2015**, *21* (52), 19243−19249.
(62) Griffiths, J. *Colour and Constitution of Organic Molecules*; Academic Press, 1976.
(63) Dewar, M. J. S. Colour and constitution. Part I. Basic dyes. *J. Chem. Soc.* **1950**, *478* (0), 2329−2334.
(64) Dewar, M. J. S.; Dougherty, R. C. *The PMO Theory of Organic Chemistry*, 1st ed.; Plenum Press: New York, 1975.
(65) Griffiths, J. Recent Developments in the Colour and Constitution of Organic Dyes. *Rev. Prog. Color. Relat. Top.* **1981**, *11* (1), 37−57.
(66) Fulmer, G. R.; Miller, A. J. M.; Sherden, N. H.; Gottlieb, H. E.; Nudelman, A.; Stoltz, B. M.; Bercaw, J. E.; Goldberg, K. I. NMR Chemical Shifts of Trace Impurities: Common Laboratory Solvents, Organics, and Gases in Deuterated Solvents Relevant to the Organometallic Chemist. *Organometallics* **2010**, *29* (9), 2176−2179.
(67) Aranzaes, J. R.; Daniel, M.-C.; Astruc, D. Metallocenes as references for the determination of redox potentials by cyclic voltammetry — Permethylated iron and cobalt sandwich complexes, inhibition by polyamine dendrimers, and the role of hydroxy-containing ferrocenes. *Can. J. Chem.* **2006**, *84* (2), 288−299.
(68) Würth, C.; Grabolle, M.; Pauli, J.; Spieles, M.; Resch-Genger, U. Relative and absolute determination of fluorescence quantum yields of transparent samples. *Nat. Protoc.* **2013**, *8* (8), 1535−1550.
(69) Rurack, K.; Spieles, M. Fluorescence Quantum Yields of a Series of Red and Near-Infrared Dyes Emitting at 600−1000 nm. *Anal. Chem.* **2011**, *83* (4), 1232−1242.
(70) Frisch, M. J.; Trucks, G. W.; Schlegel, H. B.; Scuseria, G. E.; Robb, M. A.; Cheeseman, J. R.; Scalmani, G.; Barone, V.; Mennucci, B.; Petersson, G. A.; Nakatsuji, H.; Caricato, M.; Li, X.; Hratchian, H. P.; Izmaylov, A. F.; Bloino, J.; Zheng, G.; Sonnenberg, J. L.; Hada, M.; Ehara, M.; Toyota, K.; Fukuda, R.; Hasegawa, J.; Ishida, M.; Nakajima, T.; Honda, Y.; Kitao, O.; Nakai, H.; Vreven, T.; Montgomery, J. A., Jr.; Peralta, J. E.; Ogliaro, F.; Bearpark, M. J.; Heyd, J.; Brothers, E. N.; Kudin, K. N.; Staroverov, V. N.; Kobayashi, R.; Normand, J.; Raghavachari, K.; Rendell, A. P.; Burant, J. C.; Iyengar, S. S.; Tomasi, J.; Cossi, M.; Rega, N.; Millam, N. J.; Klene, M.; Knox, J. E.; Cross, J. B.; Bakken, V.; Adamo, C.; Jaramillo, J.; Gomperts, R.; Stratmann, R. E.; Yazyev, O.; Austin, A. J.; Cammi, R.; Pomelli, C.; Ochterski, J. W.; Martin, R. L.; Morokuma, K.; Zakrzewski, V. G.; Voth, G. A.; Salvador, P.; Dannenberg, J. J.; Dapprich, S.; Daniels, A. D.; Farkas, Ö.; Foresman, J. B.; Ortiz, J. V.; Cioslowski, J.; Fox, D. J. *Gaussian 09*; Gaussian, Inc.: Wallingford, CT, 2009.
(71) Wada, M.; Konishi, H.; Kirishima, K.; Takeuchi, H.; Natsume, S.; Erabi, T. Unusual stabilities and reactivities of tris- and bis(2,4,6-trimethoxyphenyl)carbenium salts. *Bull. Chem. Soc. Jpn.* **1997**, *70* (11), 2737−2741.

DOI: 10.1021/acs.joc.8b02978
J. Org. Chem. 2019, 84, 2556−2567